Molecular Therapy
Original Article

KIM-1 augments hypoxia-induced tubulointerstitial inflammation through uptake of small extracellular vesicles by tubular epithelial cells

Jun Chen,[1,2] Tao-Tao Tang,[1,2] Jing-Yuan Cao,[1] Zuo-Lin Li,[1] Xin Zhong,[1] Yi Wen,[1] An-Ran Shen,[1] Bi-Cheng Liu,[1] and Lin-Li Lv[1]

[1]Institute of Nephrology, Zhong Da Hospital, Southeast University School of Medicine, 87 Ding Jia Qiao Road, Nanjing 210009, China

Tubular epithelial cells (TECs) exposed to hypoxia incite tubulointerstitial inflammation (TII), while the exact mechanism is unclear. In this study, we identified that hypoxia evoked tubule injury as evidenced by tubular hypoxia-inducible factor-1α and kidney injury molecule-1 (KIM-1) expression and that renal small extracellular vesicle (sEV) production was increased with the development of TII after ischemia-reperfusion injury (IRI). Intriguingly, KIM-1-positive tubules were surrounded by macrophages and co-localized with sEVs. *In vitro*, KIM-1 expression and sEV release were increased in hypoxic TECs and the hypoxia-induced inflammatory response was ameliorated when *KIM-1* or *Rab27a*, a master regulator of sEV secretion, was silenced. Furthermore, KIM-1 was identified to mediate hypoxic TEC-derived sEV (Hypo-sEV) uptake by TECs. Phosphatidylserine (PS), a ligand of KIM-1, was present in Hypo-sEVs as detected by nanoflow cytometry. Correspondingly, the inflammatory response induced by exogenous Hypo-sEVs was attenuated when *KIM-1* was knocked down. *In vivo*, exogenous-applied Hypo-sEVs localized to KIM-1-positive tubules and exacerbated TII in IRI mice. Our study demonstrated that KIM-1 expressed by injured tubules mediated sEV uptake via recognizing PS, which participated in the amplification of tubule inflammation induced by hypoxia, leading to the development of TII in ischemic acute kidney injury.

INTRODUCTION

Acute kidney injury (AKI) is an expanding serious public health problem with high morbidity and mortality, as well as an increased risk of progression to chronic kidney disease.[1,2] Despite extensive research, the pathogenesis of AKI is still largely unknown. Tubulointerstitial inflammation (TII) represents the common histological characteristic of acute and chronic kidney injury, which determines the outcome of renal disease.[3-5] Renal tubules, the main component of the kidney, are vulnerable to varieties of injuries, especially hypoxia.[6] The response of tubular epithelial cells (TECs) to injury is considered to be a key determinant of TII progression.[7] Injured TECs undergo a process of cellular and molecular changes and act as not only a passive victim of injury, but also a driving force of TII.[7] Thus, understanding the pathophysiological changes of TECs after injury may provide new insights into the mechanism of TII in AKI.

Extracellular vesicles (EVs) have received considerable attention for their potential to mediate intercellular cross-talk and contribute to the pathogenesis of kidney disease.[8,9] Fibroblasts can be activated after internalization of hypoxic TEC-derived exosomes containing *TGF-β1* mRNA and initiate renal fibrosis.[10] Macrophages uptake of exosomes from BSA-treated TECs result in an enhanced inflammatory reaction and migration of the recipient macrophages.[11] Hence, EVs are emerging as new signal vectors released by injured TECs that communicate with interstitial cells. However, whether TEC-derived EVs can act on tubules themselves and thereby augment TII remains unknown.

Kidney injury molecule-1 (KIM-1), also known as T cell immunoglobulin mucin domains-1, is an immunoglobulin superfamily protein that consists of an extracellular region, a transmembrane region and an intracellular tail.[12,13] Although virtually undetectable in normal kidneys, KIM-1 is upregulated predominantly at the apical membrane of the proximal tubules suffering from acute or chronic kidney injury.[14,15] KIM-1 is able to serve as a scavenger receptor to clear apoptotic cells to protect against AKI.[16] In contrast, KIM-1-mediated uptake of PA-albumin induces TEC pro-inflammatory response and death.[17] High urinary KIM-1 also indicates an increased possibility of severe kidney injury and predicts a poor long-term renal prognosis.[18] Therefore, the exact role of KIM-1 in the progression of TII remains obscure. Interestingly, KIM-1 is capable of recognize phosphatidylserine (PS) displayed on apoptotic cell surface,[19] which is also commonly detected as an important lipid component of

Received 17 March 2022; accepted 12 August 2022;
https://doi.org/10.1016/j.ymthe.2022.08.013.

[2]These authors contributed equally

Correspondence: Bi-Cheng Liu, Institute of Nephrology, Zhong Da Hospital, Southeast University School of Medicine, 87 Ding Jia Qiao Road, Nanjing 210009, China.
E-mail: liubc64@163.com
Correspondence: Lin-Li Lv, Institute of Nephrology, Zhong Da Hospital, Southeast University School of Medicine, 87 Ding Jia Qiao Road, Nanjing 210009, China.
E-mail: lvlinli@seu.edu.cn

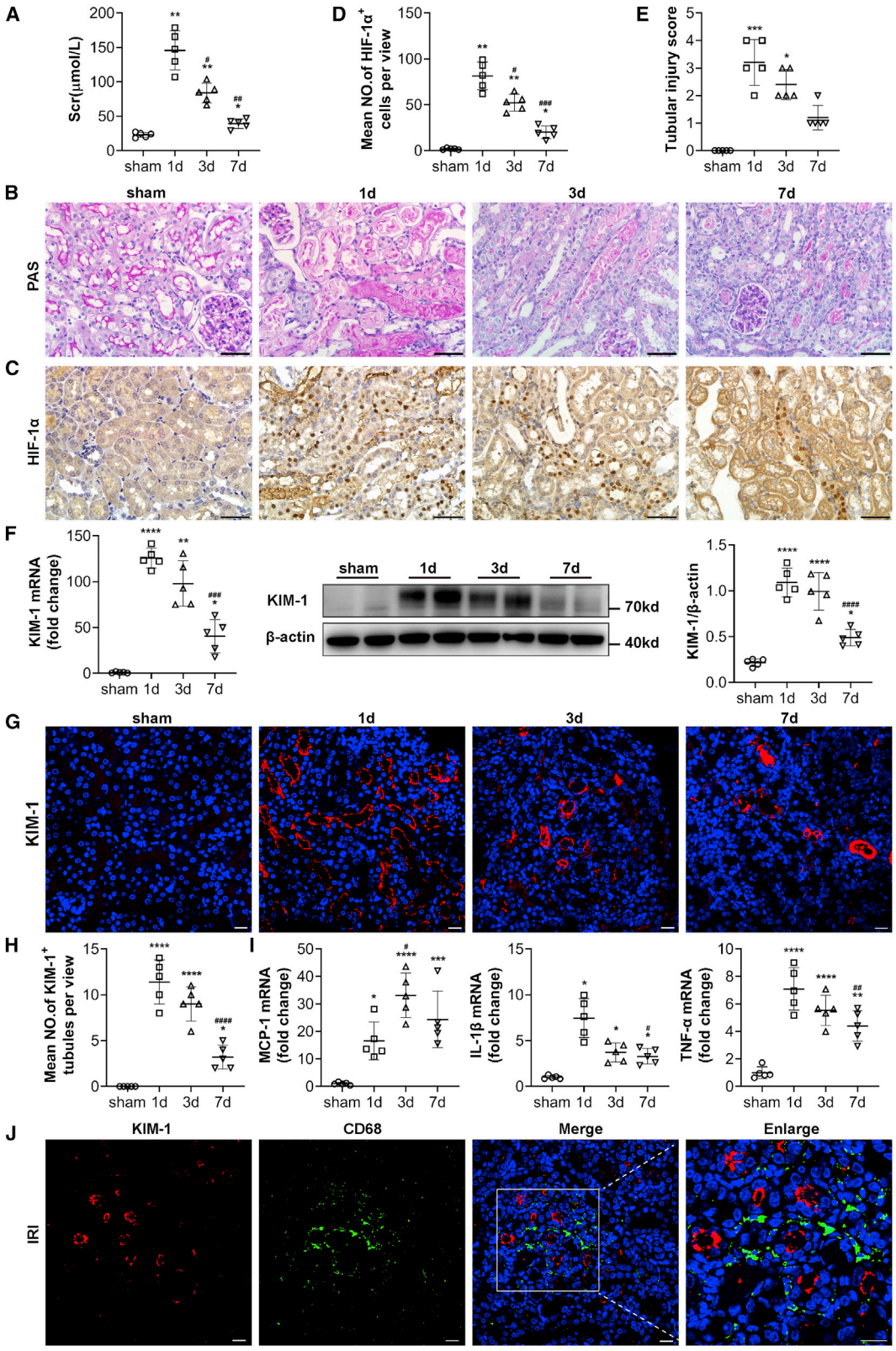

(legend on next page)

EVs.[20] However, whether EVs derived from injured TECs harbor externalized PS and its potential role in EV-mediated tubule communication remains unclear.

In this study, we demonstrated that KIM-1 expressed by injured TECs mediated the uptake of small EVs (sEVs) via recognizing PS, which consequently amplified TII induced by hypoxia. Thus, our study provides a novel insight into the mechanism of hypoxia-induced tubule injury and TII mediated by sEVs.

RESULTS

KIM-1 expression correlates with TII in ischemic AKI

Ischemia-reperfusion injury (IRI) was established to explore the conditions of hypoxia-induced inflammation as well as the expression of tubular KIM-1. Kidney function was impaired as evidenced by increased levels of serum creatinine (Scr) in IRI-induced mice on day 1 and recovered partially thereafter (Figure 1A). As shown in Figure 1B, necrosis and detachment of TECs, cellular debris accumulation, and casts formation were observed in the IRI group. HIF-1α, a marker of hypoxia, was strongly upregulated 1 day after IRI and fell thereafter, but remained elevated on day 7 (Figures 1C and 1D). Dynamic studies showed that tubular injury (Figure 1E) and KIM-1 expression (Figures 1F–1H) followed a similar pattern, along with the persistence of renal hypoxia. Concomitantly, inflammatory cytokines and chemokines including monocyte chemoattractant protein-1 (*MCP-1*), interleukin-1β (*IL-1β*) and tumor necrosis factor alpha (*TNF-α*) were also upregulated and sustained until day 7 in IRI-induced kidneys (Figure 1I). Interestingly, injured tubules with KIM-1 predominantly expressed on the apical portion were surrounded by $CD68^+$ macrophages (Figure 1J). Thus, in IRI-induced mice, persistent renal hypoxia and tubular injury coexisted with sustained KIM-1 expression and TII, which indicated a potential link between KIM-1 expression and TII under hypoxic condition.

KIM-1 mediates the pro-inflammatory response of hypoxic TECs

To further explore the correlation of elevated KIM-1 expression and pro-inflammatory response induced by hypoxia, we subjected TECs to hypoxia *in vitro*. The cells were exposed to 1% oxygen for 48 h to induce injury as previously reported[21] and the hypoxic condition was confirmed by stable HIF-1α expression in TECs (Figures 2A and 2B). In response to oxygen deprivation, KIM-1 (Figures 2C and 2D) and inflammatory cytokines (*MCP-1*, *TNF-α* and *IL-6*) expression (Figure 2E) were significantly increased in TECs. To figure out the relationship between KIM-1 expression and inflammatory cytokine elevation, *KIM-1* in hypoxic TECs was blunted by small interfering RNA (siRNA) transfection and the knockdown efficiency was assessed by quantitative real-time PCR and western blotting (Figure 2F). As a proof of principle, a decreased pro-inflammatory response was observed in TECs with KIM-1 silence, as confirmed by quantitative real-time PCR detection of *MCP-1*, *TNF-α*, and *IL-6* (Figure 2G). The data presented here demonstrated that KIM-1 contributed to the pro-inflammatory response of TECs suffering hypoxia injury, providing a rationale for enhanced infiltration of inflammatory cells around KIM-1-expressing tubules in IRI kidney (Figure 1J).

sEVs augment pro-inflammatory response of TECs induced by hypoxia and co-localize with tubular KIM-1

Next, we investigated the role of endogenous sEVs in the pro-inflammatory response of TECs to hypoxia. We first examined the impact of hypoxia on sEV secretion of TECs. sEVs were isolated and purified from the supernatant of TECs that were exposed to normoxia (Normo-sEVs) or hypoxia (Hypo-sEVs) (Figure 3A). Electron microscopy revealed the presence of sEVs with morphology of bilayer cup-shape (Figure 3B). Nanoflow cytometry (nFCM) showed that the average diameter of sEVs was approximately 73 nm (Figure 3C) and verified that more sEVs were released by hypoxia-treated TECs than normoxia-exposed (Figure 3D), which was further confirmed by BCA assay of sEV total protein (Figure 3E) and western blotting analysis of sEV markers (TSG101, ALIX, and CD63) (Figure 3F). To interrogate the roles of sEVs in hypoxia-induced pro-inflammatory effect of TECs, siRNA against *Rab27a*, a small guanosine triphosphatase involved in regulating sEV secretion as we previously reported,[22] was used to silence Rab27a expression (Figure 3G), which resulted in decreased sEV secretion by hypoxic TECs (Figures 3H and 3I). Notably, the inhibition of sEV secretion significantly decreased *MCP-1* expression in hypoxic TECs (Figure 3J). Meanwhile, in hypoxic TECs, treatment of exogenous Hypo-sEVs increased *MCP-1* expression compared with Normo-sEVs (Figure 3K). Furthermore, we examined the sEV production in kidneys of bilateral IRI-induced AKI mice. Consistently, electron microscopy revealed that the morphology of sEVs isolated from kidney tissues resembled that from TECs (Figure 3L). Compared with sham, ischemic kidneys exhibited increased sEV production as measured by CD63 protein in extracted sEVs (Figure 3M). In fact, as shown in Figure 3N, the majority of renal sEVs were produced by TECs as evidenced by immunofluorescence detection of CD63 expression. Impressively, we noticed the co-localization of CD63 and KIM-1 (Figure 3O), which suggested an increased sEV production in injured tubules or uptake of sEVs by damaged tubules through KIM-1. Thus,

Figure 1. KIM-1 expression correlates with TII in ischemic AKI

(A) Scr of sham and bilateral IRI-induced mice. (B) Periodic acid-Schiff staining of kidney sections from sham and IRI-induced mice. Scale bars, 50 μm. (C) HIF-1α immunohistochemistry of kidney sections from sham and IRI mice. Scale bars, 50 μm. (D) Quantification of HIF-1α positive TECs according to HIF-1α immunohistochemistry. (E) Quantitative analysis of tubular injury according to periodic acid-Schiff staining. (F) Quantitative real-time PCR and western blotting analysis of KIM-1 expression in kidneys. (G) Immunofluorescent staining of KIM-1 in kidneys. Scale bars, 20 μm. (H) Quantification of KIM-1-positive tubules in kidneys according to immunofluorescent staining. (I) Quantitative real-time PCR analysis of inflammatory cytokines in kidneys. (J) Co-staining for CD68 (green) and KIM-1 (red) in the kidney 7 days after IRI. Scale bars, 20 μm. Data are presented as mean ± standard deviation for each group of mice (n = 5). *p < 0.05, **p < 0.01, ***p < 0.001, ****p < 0.0001 versus sham; #p < 0.05, ##p < 0.01, ###p < 0.001, ####p < 0.0001 versus 1 day, one-way ANOVA.

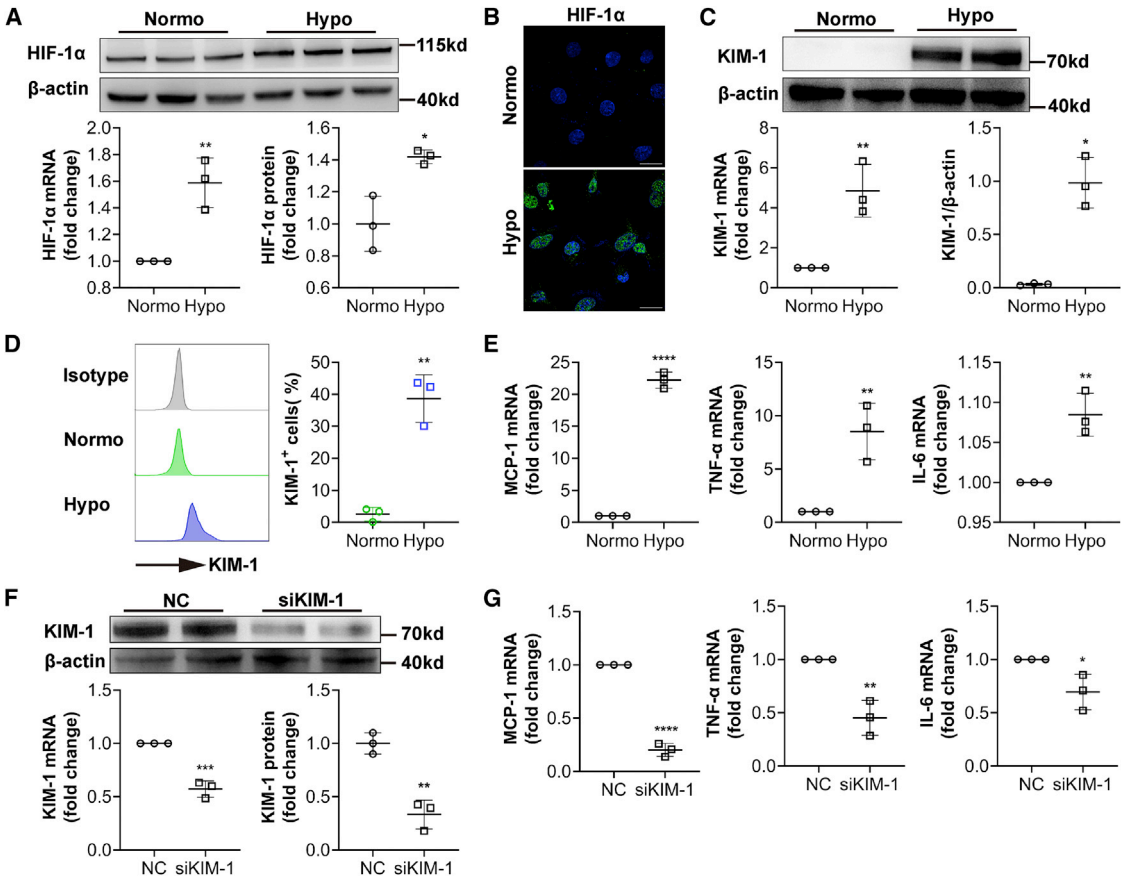

Figure 2. KIM-1 mediates the pro-inflammatory response of hypoxic TECs

(A) Quantitative real-time PCR and western blotting analysis of HIF-1α expression in normoxic (Normo) and hypoxic (Hypo) TECs. (B) Immunofluorescent staining of HIF-1α in TECs. Scale bars, 20 μm. (C) Quantitative real-time PCR and western blotting analysis of KIM-1 expression in TECs. (D) Flow cytometry analysis of KIM-1 expression in TECs. (E) Quantitative real-time PCR analysis of inflammatory cytokine production in TECs. (F) Quantitative real-time PCR and western blotting analysis of the knockdown efficiency of KIM-1 in TECs under hypoxic condition. (G) Quantitative real-time PCR analysis of inflammatory cytokine production in TECs with siKIM-1 or negative control (NC) transfection under hypoxic condition. Data are presented as mean ± standard deviation for each group (n = 3). *p < 0.05, **p < 0.01, ***p < 0.001, ****p < 0.0001 versus Normo (A, C, D and E) or NC (F and G), two-tailed *t* test.

hypoxic TECs produced a substantial higher number of sEVs with the capacity to amplify the inflammation of the tubules.

KIM-1/PS-mediated Hypo-sEV uptake aggravates the inflammation of TECs

To clarify whether KIM-1 is responsible for the sEV-mediated TEC pro-inflammatory response, we overexpressed KIM-1 in TECs via lentiviral transduction. As shown in Figures 4A and 4B, KIM-1 was efficiently overexpressed and more than 90% of TECs were KIM-1 positive. To assess uptake efficiency, sEVs isolated and purified from DiI-stained hypoxic TECs were applied to TECs with KIM-1 transduction; Figure 4C shows the schematic diagram of the experiment design. Flow cytometry showed that the percentage of TECs taking up DiI-labeled sEVs is higher in the group of KIM-1 overexpression compared with the NC group (Figure 4D). Consistently, confocal optical microscopy demonstrated that more fluorescence-labeled sEVs accumulated in TECs in the group of KIM-1 overexpression (Figures 4E and 4F). Likely, under hypoxic conditions, TECs with KIM-1 expression avidly phagocytosed more DiI-labeled sEVs compared with KIM-1-negative cells (Figures 4G and 4H). The results indicated that KIM-1 enhanced the ability of TECs to take up sEVs. Importantly, in hypoxic TECs, exogenous Hypo-sEV-induced increased the production of inflammatory cytokines (*MCP-1*, *TNF-α*, and *IL-6*) could be partly reversed when *KIM-1* was knocked down by siRNA transfection (Figure 4I), indicating that Hypo-sEVs promoted TEC pro-inflammatory response in a KIM-1-dependent manner. Of note, PS, which was recognized as the dominant membrane lipid that could be recognized by KIM-1, was readily detected in Hypo-sEVs by fluorescein isothiocyanate (FITC)-conjugated annexin V via nFCM (Figure 4J). Overall, these findings suggested that sEVs accelerated the inflammation of TECs via KIM-1-mediated vesicle uptake through recognizing PS.

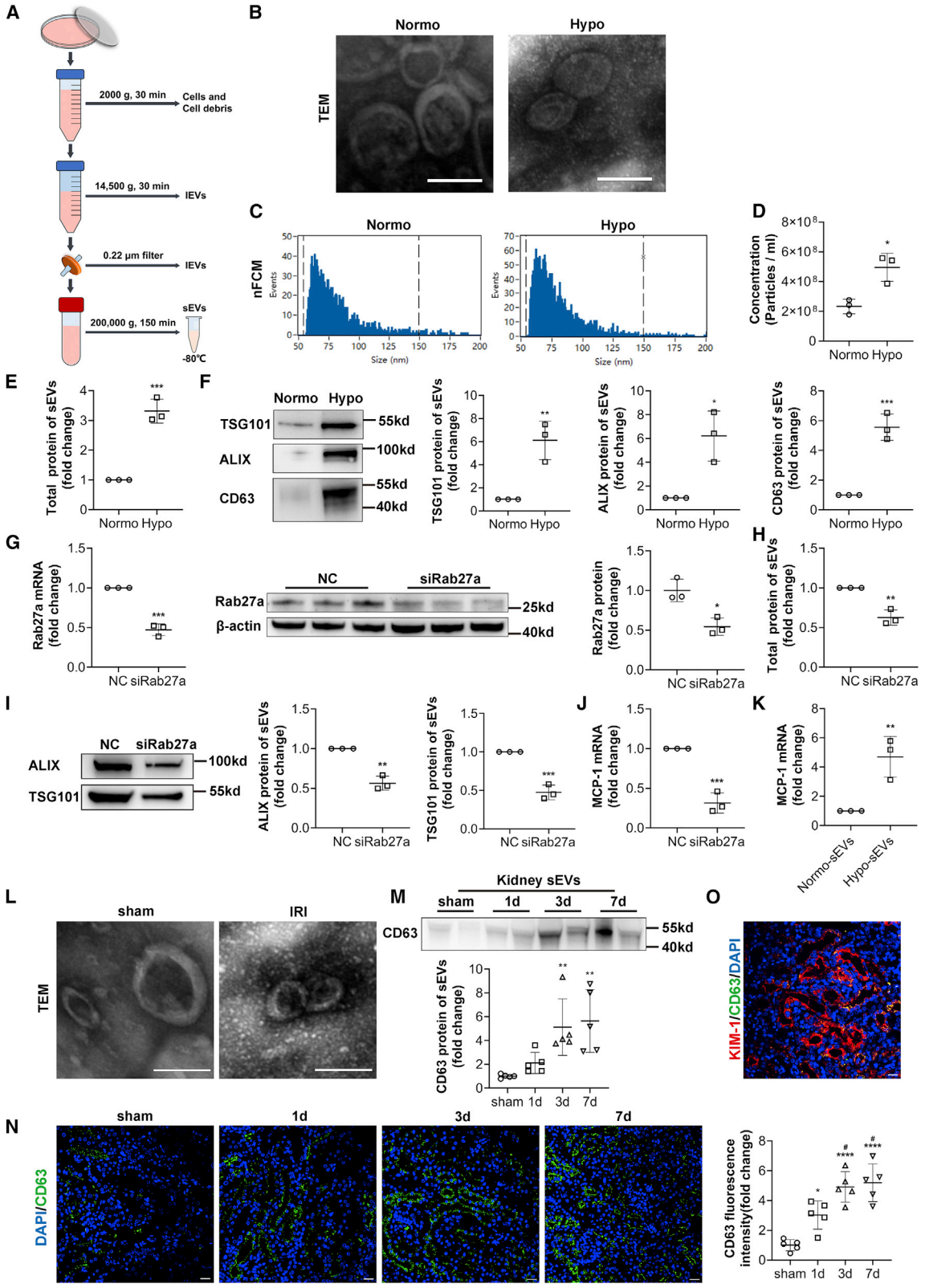

(legend on next page)

KIM-1-mediated Hypo-sEV uptake amplifies TII in IRI mice

To further investigate whether KIM-1 is responsible for sEV uptake *in vivo*, we generated a unilateral IRI mouse model to induce KIM-1 expression in injured tubules. We intravenously injected DiI-labeled Hypo-sEVs at 24 h after IRI when KIM-1 expression was significantly upregulated. *Ex vivo* imaging of the kidney was performed at 6 h after injection. Compared with sham kidneys, remarkably higher renal radiation signals were observed in IRI-induced kidneys (Figure 5A). Furthermore, DiI-labeled Hypo-sEVs preferred to deposit in IRI-induced kidneys, especially in the renal tubules, which was confirmed by confocal microscopy (Figure 5B). Moreover, DiI-labeled Hypo-sEVs were noticed to localize to KIM-1-positive tubules (Figure 5C), which indicated internalization of Hypo-sEVs by injured tubules via KIM-1.

To explore the capacity of the Hypo-sEVs in aggravating the inflammatory response of bilateral IRI-induced kidney, Hypo-sEVs and Normo-sEVs were injected into kidneys after reperfusion. Mice were sacrificed at 24 h after sEV injection. Renal inflammatory cytokines (*MCP-1*, *TNF-a*, *IL-1β*, and *IL-6*) were upregulated in Hypo-sEV-injected kidneys compared with that Normo-sEV-injected (Figure 5D). Moreover, Hypo-sEVs also aggravated TII evidenced by $CD68^+$ macrophages and $CD3^+$ T cells infiltration (Figure 5E). More important, Hypo-sEV-treated mice showed stronger MCP-1 (Figure 5F) expression in KIM-1-positive tubules compared with Normo-sEV-treated mice. These results suggested that the sEVs released by hypoxia-treated TECs could be taken up by KIM-1-expressing TECs, which subsequently amplified TII.

DISCUSSION

Tubular injury is a vital hallmark shared by various kidney injuries and tightly linked with the outcome of renal disease.[23] Injured TECs undergo many pathophysiological changes, of which KIM-1 elevation is prominent. Beyond its initial recognition as a biomarker of renal disease,[24] KIM-1 is increasingly considered to be associated with tubulointerstitial lesions and progression to kidney failure,[25] but the underling mechanism is elusive. Our previous study has identified that EV-mediated communication between injured TECs and inflammatory cells plays essential pathologic roles in TII.[3] However, the role of sEVs in the communication of injured TECs is unclear. In this study, we demonstrated that KIM-1 acted as a tubular receptor for sEV uptake, which promoted the transmission and amplification of inflammatory signaling among injured tubules, leading to the development of TII (Figure 6). The study presented here sheds new lights on the pathophysiology of TII.

Renal hypoxia that occurs in many types of kidney injury contributes to the development of TII,[26,27] but the underling mechanism has yet to be determined. Interestingly, KIM-1 expression is closely linked to hypoxia, and KIM-1 expression is found to be prominent in areas of decreased capillary density in IgA nephropathy.[28] In this study, we found that KIM-1-positive tubules were surrounded by inflammatory cells in ischemic AKI, and silence of KIM-1 decreased the inflammatory cytokine expression in hypoxia-treated TECs. A recent study has demonstrated that the conditional expression of KIM-1 in TECs in the absence of an injury factor leads to spontaneous and progressive interstitial renal inflammation.[29] Therefore, KIM-1 expression can lead to the activation of inflammatory signaling by itself without injury stimulus. Meanwhile, tubule KIM-1 plays an essential role in amplifying the tubule inflammatory response induced by hypoxia and subsequent TII.

Accumulating evidence suggests that sEV is a novel messenger mediating cell-cell communication.[30,31] Our team has recently confirmed that TECs exposed to hypoxia during kidney injury communicated with macrophages via sEVs and led to TII.[21] In the current study, we found a new role for sEVs in aggravating TEC pro-inflammatory response. Rab27a is known to be involved in the regulation of EV secretion.[32,33] As expected, the inhibition of sEV release via silence of Rab27a mitigated the hypoxia-induced pro-inflammatory response of TECs. Therefore, sEVs released by hypoxic TECs augment the pro-inflammatory response of tubule after AKI.

Once released, EVs are capable of transmitting information and influencing the pathological status of recipient cells.[34] The selectivity of EVs that are recognized and internalized by recipient cells depends on the surface properties of the sEVs and target cells.[35,36] A number of related receptors and adhesion molecules on EV surface and

Figure 3. sEVs augment pro-inflammatory response of TECs induced by hypoxia and co-localize with tubular KIM-1

(A) Schematic diagram of sEV isolation and purification from TEC supernatant by series of centrifugation (lEVs, large EVs). (B) Morphology of Normo-sEVs and Hypo-sEVs under TEM. Scale bars, 100 nm. (C) Size distribution of sEVs analyzed by nFCM. (D) sEV concentration quantified by nFCM considering the resuspension volumes and dilution factors (n = 3). *p < 0.05 versus Normo. (E) Quantification of sEV total protein by BCA assay (n = 3). ***p < 0.001 versus Normo. (F) Characterization and quantification of sEVs by western blotting analysis of sEV markers (n = 3). *p < 0.05, **p < 0.01, ***p < 0.001 versus Normo. (G) Quantitative real-time PCR and western blotting analysis of the knockdown efficiency of Rab27a in TECs under hypoxic condition. (n = 3). *p < 0.05, ***p < 0.001 versus NC. (H) BCA assay of total protein in sEVs from cultured supernatant of TECs with NC or siRab27a transfection (n = 3). **p < 0.01 versus NC. (I) Characterization and quantification of sEVs by western blotting analysis of sEV markers (n = 3). **p < 0.01, ***p < 0.001 versus NC. (J) Quantitative real-time PCR analysis of MCP-1 in hypoxic TECs with siRab27a or NC transfection(n = 3). ***p < 0.001 versus NC. (K) Quantitative real-time PCR analysis of MCP-1 in hypoxic TECs cocultured with Hypo-sEVs (n = 3). **p < 0.01 versus Normo-sEVs.

(L) Morphology of sEVs derived from kidney tissues under TEM. Scale bars, 100 nm.

(M) Western blotting analysis of CD63 expression in sEVs extracted from kidney tissues of sham and bilateral IRI-induced mice (n = 5). **p < 0.01 versus sham.

(N) Immunofluorescent staining and quantification of CD63 in kidney sections from sham and bilateral IRI-induced mice (n = 5). Scale bars, 20 μm. *p < 0.05, ****p < 0.0001 versus sham; #p < 0.05 versus 1 day.

(O) Co-staining for CD63 (green) and KIM-1 (red) in IRI-induced kidney. Scale bar, 20 μm. Data are presented as mean ± standard deviation for each group. Two-tailed *t* test (D, E, F, G, H, I, J and K), one-way ANOVA (M and N).

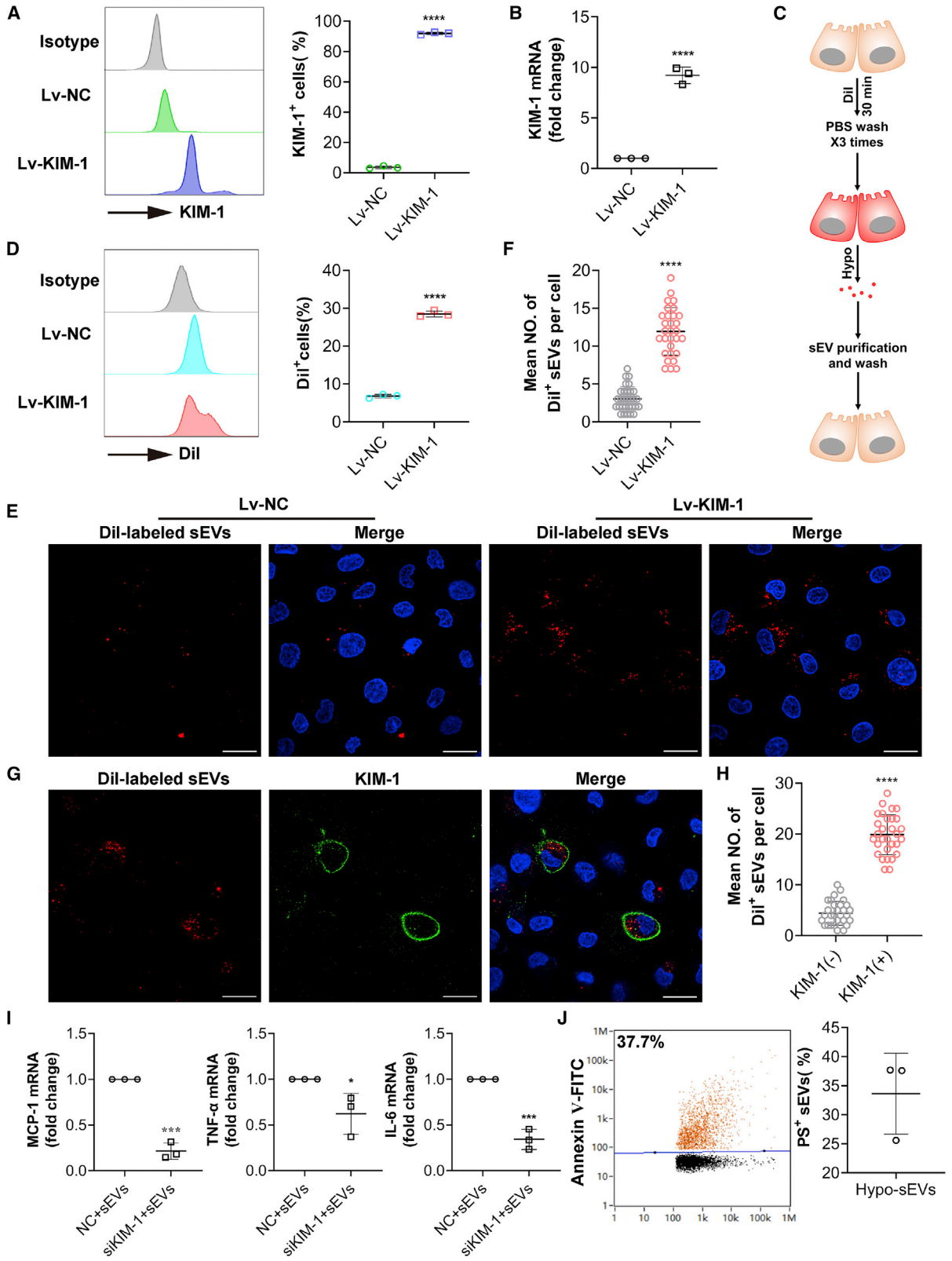

(legend on next page)

recipient cells have been identified, including tetraspanins, integrins, proteoglycans, lectins, lipids, intercellular adhesion molecules and extracellular matrix components.[37,38] KIM-1 is originally identified as an early biomarker of renal proximal tubule injury. Recently, it has been confirmed that KIM-1 can function as a receptor recognizing PS,[39] oxidized low-density lipoprotein,[39] LMIR5/CD300b,[40] apoptosis inhibitor of macrophage,[41] and fatty acid.[17] In the current study, KIM-1 acted as a membrane receptor for sEV uptake by recognizing PS on the surface of vesicles released by hypoxic tubules. More important, silence of KIM-1 in hypoxic TECs dampened the pro-inflammatory response induced by exogenous Hypo-sEVs. The cargos of the sEVs are also responsible for the pro-inflammatory response of recipient TECs. Previous studies have revealed that the contents of EVs change along with the status of their parental cells.[42,43] EVs shed from hypoxic cells are specifically loaded with complement (e.g., C3),[44] cytokines (including CSF-1, CCL2, TGF-β, TNF-α, and IL-32),[45-47] and pro-inflammatory microRNA (e.g., *miR-23a*).[21] EV-mediated delivery of pro-inflammatory components among TECs may contribute to the aggravation of TEC pro-inflammatory response. Hence, KIM-1 expressed on the membrane of the hypoxic TECs facilitated recognition of vesicle PS and internalization of the Hypo-sEVs, which promoted hypoxia-induced TII.

In parallel, exogenous Hypo-sEVs tended to target injured kidneys and preferentially localized to tubules with KIM-1 expression. Additionally, Hypo-sEVs administration increased the expression of inflammatory factors and infiltration of inflammatory cells in IRI-induced kidneys. More important, KIM-1$^+$ tubules in Hypo-sEV-treated mice acquired an enhanced pro-inflammatory phenotype. We have recently demonstrated that KIM-1 can recognize EVs modified with KIM-1-binding LTH peptide and promote the accumulation of therapeutic EVs to injured tubules.[48] The data provided here further validated that KIM-1 could mediate endogenous sEV uptake and subsequently aggravate TII. However, some studies found that KIM-1-mediated uptake of apoptotic cell bodies can downregulate nuclear factor-κB activation and decrease inflammation during the early stage of AKI.[16] Thus, it seems that KIM-1acts as a double-edged sword and harbors multiple roles in kidney injury and repair, and the downstream effects of KIM-1-mediated phagocytosis may depend on the components taken up by TECs. Clinically, among patients with pre-existing chronic kidney disease (CKD), AKI during hospitalization is associated with long-term elevation in plasma KIM-1 after the acute insult, which may contribute to the chronic loss of renal function.[49] Children with higher urine KIM-1 concentrations are at significantly higher risk of CKD progression compared with groups with lower levels.[50] It is worth noting that tubular KIM-1 expression and sEV production remained elevated on day 7 despite the partial remission of renal dysfunction, indicating that KIM-1-expressing TECs would progressively internalize sEVs from their neighboring TECs and lead to the persistence of TII. Whether KIM-1-mediated sEV uptake is engaged in AKI-to-CKD transition requires further investigation.

In summary, we have demonstrated that KIM-1 expressed by injured tubules facilitates uptake of sEVs via interaction with PS and augments hypoxia-induced TII. This study provides a new insight into the mechanism of hypoxia induced TII and may offer a potential intervention target for ischemic AKI.

MATERIALS AND METHODS

Animal models

Male C57BL/6 mice (8-10 weeks old), weighing 20–22 g, were purchased from the Beijing Vital River Laboratory Animal Technology Co., Ltd. All animal experiments were carried out in accordance with guidelines approved by our Institutional Animal Care and Use Committee and Ethics Committee of Southeast University. For the bilateral IRI, procedures were performed as previously described.[51] Briefly, both renal pedicles were clamped for 32 min and removed after the specified time and the body temperature was monitored and kept at 36.8°C–37.5°C by a sensitive rectal probe throughout the procedure. Mice were sacrificed on day 1, day 3, and day 7 after surgery and their blood was collected for creatinine determination. In addition, kidneys were harvested and processed for histology and extraction of RNA and protein. Sham operations were the same except for renal pedicle clamping. For the unilateral IRI, only the right renal pedicle was subjected to ischemia for 32 min followed by reperfusion, leaving the left kidney as an internal control without the induction of ischemia.

To specifically assess the role of EVs in TII, 40 μg of Hypo-sEVs or Normo-sEVs were respectively injected into four sites of each renal parenchyma after bilateral reperfusion. The method of renal intraparenchymal injection originated from our prior experience.[21] Mice were sacrificed 24 h after injection.

Kidney function assessment

Kidney function was estimated by determination of Scr. Scr levels were measured by a Creatinine Assay kit (Nanjing Jiancheng

Figure 4. KIM-1/PS-mediated Hypo-sEV uptake aggravates the inflammation of TECs

(A and B) Flow cytometry and quantitative real-time PCR analysis of KIM-1 expression in TECs with lentiviral transduction of KIM-1 (Lv-KIM-1) or control (Lv-NC) (n = 3). ****p < 0.0001 versus Lv-NC. (C) Schematic diagram of sEV labeling, isolation and coculture with TECs. (D) Flow cytometry analysis of cellular uptake of DiI-labeled Hypo-sEVs by TECs with Lv-KIM-1 or Lv-NC transduction (n = 3). ****p < 0.0001 versus Lv-NC. (E) Fluorescent images of DiI-labeled Hypo-sEVs phagocytosed by TECs with Lv-KIM-1 or Lv-NC transduction. Scale bars, 20 μm. (F) Mean number of DiI-labeled Hypo-sEVs internalized by TECs with Lv-KIM-1 or Lv-NC transduction. ****p < 0.0001 versus Lv-NC. (G) Fluorescent images of DiI-labeled Hypo-sEVs phagocytosed by TECs under hypoxic condition. Scale bars, 20 μm. (H) Mean number of DiI-labeled Hypo-sEVs internalized by KIM-1 positive (KIM-1$^+$) and negative (KIM-1$^-$) TECs under hypoxic condition. ****p < 0.0001 versus KIM-1$^-$. (I) The transcriptional levels of inflammatory cytokines in siKIM-1 or NC transfected hypoxic TECs cocultured with Hypo-sEVs. *p < 0.05, ***p < 0.001 versus NC + sEVs. (J) nFCM analysis of PS on the surface of Hypo-sEVs (n = 3). All Data are presented as mean ± standard deviation for each group. Two-tailed *t*-test.

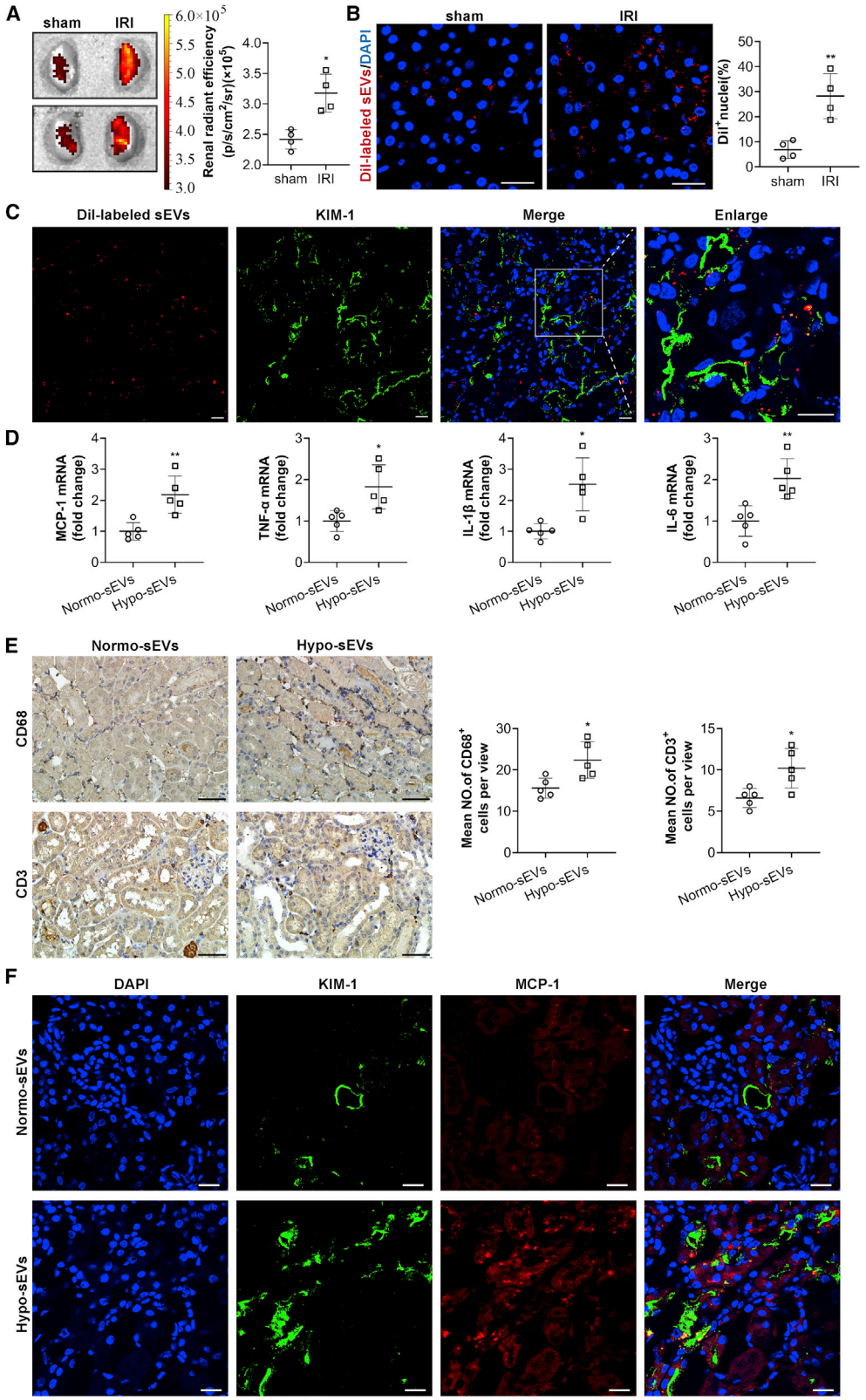

(legend on next page)

Bioengineering Institute, Nanjing, China). The levels of Scr were expressed as μmol/L.

Cell culture

The TEC cell line (immortalized mouse TECs) was a gift from J. B. Kopp, National Institutes of Health. TECs were cultured in DMEM/F12 (Gibco by Life Technologies, Grand Isle, NY, USA) supplemented with 10% fetal bovine serum (Gibco), 1% streptomycin and penicillin (Gibco by Life Technologies). The incubator conditions were maintained at 37°C with 5% CO_2 and 95% humidity.

siRNA transfection and lentiviral transduction

For siRNA-mediated knockdown, *KIM-1* siRNA or *Rab27a* siRNA against mouse was transfected into TECs when they grew to 60%–70% confluence. A scrambled sequence was selected as a negative control. The transfection was a lipofectamine-based method and performed according to the protocol provided by the manufacture (GenePharma, Shanghai, China). The sequences of siRab27a and siKIM-1 were as follows: (1) *Rab27a* siRNA: sense: GAUGCACGCGUACUGUGAATT; antisense: UUCACAGUACGCGUGCAUCTT; (2) *KIM-1* siRNA: sense: CCGUGUCUCUAAGAUUGAATT; antisense: UUCAAUCUUAGAGACACGGTT. siRNA and Lipofectamine 3000 (Invitrogen, Waltham, MA, USA) were mixed with Opti-MEM (Gibco by Life Technologies) at room temperature (RT) before being applied to cells synchronized with serum-free medium.

For lentiviral transduction, lentivirus-expressing mouse *HAVCR1* (also named *KIM-1*) gene produced by GeneChem (Shanghai, China) was seeded in TECs with a confluence of approximately 50%. After transduction, puromycin was applied to select KIM-1-overexpressing cells until they accounted for more than 90% of the infected TECs.

sEV isolation and purification

To extract TEC-derived sEVs, TECs were cultured with the DMEM/F12 medium containing 10% FBS until 80%–90% confluence and the cells were then washed with sterile phosphate-buffered saline (PBS, Solarbio Life Sciences, Beijing, China) twice. For hypoxia experiments, the cells were subjected to an incubator setting of 1% O_2 for 48 h with serum- and glucose-free DMEM/F12 medium (Procell Life Science & Technology, Wuhan, China). Before treatment, the O_2 concentration of the medium was balanced in the incubator for more than 6 h. For normoxic incubation, the cells remained in normoxic condition for 48 h with fresh serum-free medium. For Rab27a inhibition experiment, TECs were subjected to an incubator setting of 1% O_2 for 48 h with serum- and glucose-free DMEM/F12 medium (Procell Life Science & Technology) after siRab27a transfection. The resultant supernatant fractions were collected and submitted for sEV extraction. To isolate sEVs from kidney, as previously reported,[22] 100 mg renal cortex was dissected and digested with DMEM solution containing collagenase and trypsin for 2 h at 37°C. Then the enzymes were neutralized with exosome-free FBS and the homogenate was harvested for sEV extraction. sEVs were extracted by a set of centrifugation procedures. Briefly, the samples were centrifuged at 2,000×*g* for 30 min to remove the cells and debris, then centrifuged at 14,500×*g* for 30 min and subjected to filtration on 0.22-μm pore filters to eliminate large EVs (lEVs), followed by ultracentrifugation at 200,000×*g* for 150 min (70Ti, Optima XPN-100 Ultracentrifuge, Beckman Coulter, Pasadena, CA, USA). The sEV pellets were resuspended in PBS and collected by ultracentrifugation at 200,000×*g* for 150 min again. Purified sEVs were diluted in PBS and preserved at −80°C.

Transmission electron microscope

For transmission electron microscope (TEM) viewing, sEV samples were diluted 1:1 with PBS buffer and then applied on 200-mesh nickel grids and standed for 20 min followed by stained with 1% uranyl acetate solution for 5 min at RT, and then air dried. The samples were observed and imaged with TEM (H-7650, Hitachi, Tokyo, Japan) at 80 kV.

Nanoflow cytometric analysis

The size distribution and concentration of sEVs were assayed by nanoFCM (U30, Xiamen Fuliu Biological Technology, Xiamen, China). For phenotyping of PS, Annexin V FITC (556,547, BD Pharmingen, San Diego, CA, USA) was used. To be brief, sEVs isolated and purified from supernatants of cultured hypoxic TECs by centrifugation were resuspended in binding buffer at a proper concentration, followed by Annexin V FITC incubation. The mixture was then washed twice with binding buffer through ultracentrifugation at 200,000×*g* for 150 min at 4°C. The sEV pellets were resuspended for nFCM analysis.

sEV labeling

To obtain fluorescence-labeled sEVs, the TECs were incubated with 1,1′-dioctadecyl-3,3,3′,3′-tetramethylindocarbocyanine perchlorate (DiI, C1036, Beyotime Biotechnology, Shanghai, China) for 30 min and washed three times with sterile PBS to eliminate free dye. The labeled cells were placed in hypoxic circumstance for 48 h with a serum- and glucose-free culture medium. The resultant supernatant fractions were collected and submitted for sEV extraction using centrifugation.

Figure 5. KIM-1-mediated Hypo-sEV uptake amplifies TII in IRI mice

(A) Fluorescence intensity imaging of bilateral kidneys collected from unilateral IRI-induced mice after intravenous administration of DiI-labeled Hypo-sEVs (n = 4). *p < 0.05 versus sham. (B) Fluorescent images of kidney sections with DiI-labeled Hypo-sEVs accumulation (n = 4). Scale bars, 20 μm. **p < 0.01 versus sham. (C) Fluorescent images of KIM-1 co-localizing with DiI-labeled Hypo-sEVs in IRI-induced kidney. Scale bars, 20 μm. (D) Quantitative real-time PCR analysis of inflammatory cytokines in bilateral IRI-induced kidneys after local injection of Normo-sEVs or Hypo-sEVs (n = 5). *p < 0.05, **p < 0.01 versus Normo-sEVs. (E) Immunohistochemistry for $CD68^+$ macrophages and $CD3^+$ T cells in kidneys with local injection of Normo-sEVs or Hypo-sEVs (n = 5). Scale bars, 50 μm. *p < 0.05 versus Normo-sEVs. (F) Co-staining for MCP-1(red) and KIM-1 (green) in kidneys with local injection of Normo-sEVs or Hypo-sEVs. Scale bars, 20 μm. Data are presented as mean ± standard deviation for each group. Two-tailed *t* test.

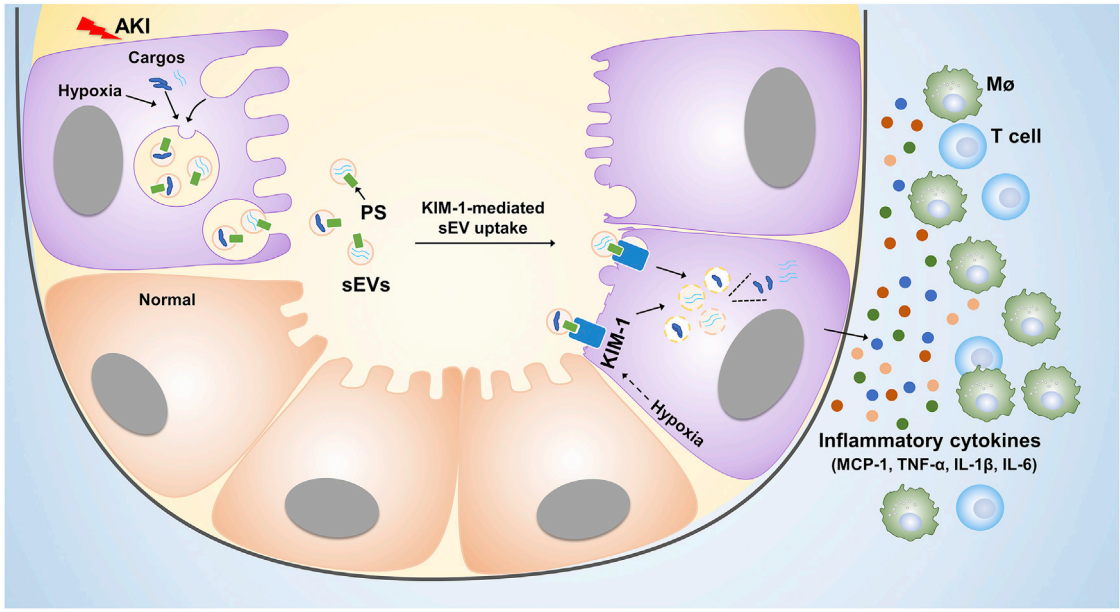

Figure 6. Schematic illustration of KIM-1-mediated sEV uptake aggravating TII induced by hypoxia

In IRI mice, hypoxia-injured tubules release PS-displayed sEVs, which are internalized by neighboring or distant hypoxia-injured tubules via KIM-1. Subsequently, tubules activated by Hypo-sEVs secrete more inflammatory cytokines to recruit inflammatory cells, which augments TII. In summary, TECs communicate through KIM-1-mediated sEV uptake, leading to the spread of the injury signal and promoting the progression of TII. Mø, macrophages; MCP-1, monocyte chemoattractant protein-1.

Cellular uptake of sEVs *in vitro*

To explore the role of KIM-1 in sEV-mediated tubule communication, DiI-labeled sEVs were applied to culture TECs under hypoxic condition and TECs with KIM-1 transduction. Two hours after that, the cells were washed with sterile PBS three times to eliminate free sEVs. Then the group of cells with KIM-1 transduction were collected and detected by flow cytometry (BD, San Jose, CA, USA). Alternatively, the cells were fixed with paraformaldehyde and stained with DAPI Staining Solution (Beyotime Biotechnology) followed by observation through confocal microscope (FV1000, Olympus, Tokyo, Japan). The number of DiI-labeled sEVs internalized by each cell was counted and averaged.

In vivo biodistribution of sEVs

To evaluate the distribution of sEVs in the kidney, DiI-labeled Hypo-sEVs (100 μg) were administered intravenously into mice 24 h after unilateral IRI. Kidneys were harvested and imaged under the same conditions with the aid of IVIS Spectrum imaging system (PerkinElmer, Waltham MA, USA) 6 h after administration. Afterward, the sectioned kidney tissues were immersed in DAPI to stain nuclear, and images were viewed and captured using a confocal microscope (FV1000, Olympus). Nuclei surrounded with DiI-labeled Hypo-sEVs were counted and divided by the total number of nuclei. The average resultant data from kidney was used to quantify the distribution of Hypo-sEVs.

Histology, immunohistochemistry, immunofluorescence staining

To assess the renal injury, kidney sections embedded in paraffin were performed for periodic acid-Schiff staining. The tubular injury was quantified as follows: 0, no damage; 1, less than 25%; 2, 25%–50%; 3, 50%–75%; and 4, greater than 75%.[51] For immunohistochemistry,

Table 1. Primers for quantitative real-time PCR

Primer (Mouse)	Forward	Reverse
MCP-1	CTTCTGGGCCTGCTGTTCA	CCAGCCTACTCATTGGGATCA
IL-1β	GGTAAGTGGTTGCCCATCAGA	GTCGCTCAGGGTCACAAGAAA
TNF-α	CATCTTCTCAAAATTCGAGTGACAA	TGGGAGTAGACAAGGTACAACCC
IL-6	AAAGAGTTGTGCAATGGCAATTCT	AAGTGCATCATCGTTGTTCATACA
KIM-1	TCAGAAGAGCAGTCGGTACAAC	TGTAGCTGTGGGCCTTGTAGT
HIF-1α	AGATTCTGTTTGTTGAAGGGAG	AGGTGGATATGTCTGGGTTGA
Rab27a	TTCCTGCTTCTGTTCGACCT	GCTTATGTTTGTCCCGTTGG
β-actin	GGGAAATCGTGCGTGAC	AGGCTGGAAAAGAGCCT

the kidney slides were immunostained with primary antibodies against HIF-1α (NB100-479, Novus Biologicals, Centennial, CO, USA), CD3 (ab16669, Abcam, Cambridge, UK), CD68 (ab125212, Abcam) and then analyzed using streptavidin peroxidase detection system (Maixin, Fuzhou, China) in accordance with the instructions of the manufacturer. 3,3′-diaminobenzidine (Maixin) as a horseradish peroxidase (HRP)-specific substrate was applied to the slides, which were then counter-stained with hematoxylin. Positive cells were observed and quantified in random fields under a light microscope (Olympus) and averaged per mouse.

For immunofluorescence, TECs and kidney sections were treated with 0.25% Triton X-100 and blocked with 5% BSA. The samples were reacted with primary antibodies against HIF-1α (ab228649, Abcam), KIM-1 (MA5-28211, Invitrogen, USA), CD68 (ab125212, Abcam), CD63 (ab216130, Abcam), MCP-1 (DF7577, Affinity, Changzhou, China). Subsequently, fluorescently labeled secondary antibodies were applied to the samples. Nuclei were counter-stained with DAPI. Finally, samples were scanned by confocal microscopy system (FV1000, Olympus). Quantification of positive tubules was conducted in random fields and averaged per mouse. Fluorescence intensity was analyzed through the ImageJ software (NIH, Bethesda, MD, USA).

Flow cytometry analysis

After treatment with hypoxia or Lv-KIM-1 transduction, TECs were collected and stained with CD365 (KIM-1) antibody (566,336, BD Pharmingen). Isotype control antibodies worked as negative controls. Single cells were detected by flow cytometry (BD, San Jose, CA, USA) after extensive washing. TECs cocultured with DiI-labeled HyposEVs were harvested and analyzed directly as mentioned above. FlowJo software was used to analyze data.

Quantitative RT-PCR assay

A quantitative RT-PCR was applied to test gene expression of kidney tissues and TECs. In Brief, RNAiso Plus (Vazyme, Nanjing, China) was used to extract total RNA from the samples. To obtain cDNA, total RNA was reverse transcribed using 5× HiScript III qRT SuperMix (Vazyme). PCR was performed using 2×ChamQ SYBR qPCR Master Mix (Vazyme) and 7300 PCR System (Applied Biosystems, Waltham, MA, USA). The sequences of all the primers for quantitative real-time PCR are listed in Table 1. Relative expression of the target genes was normalized to β-actin levels.

Western blotting

Renal tissues, TECs and purified sEVs were lysed on ice with cold RIPA Lysis buffer (ThermoFisher Scientific, Waltham, MA, USA) with protease inhibitor added. Protein concentration was quantified by BCA assay (KeyGEN BioTECH, Nanjing, China). Proteins were separated by SurePAGE (GenScript, Piscataway, NJ, USA) and transferred onto PVDF Transfer Membranes (ThermoFisher Scientific, Rockford, IL, USA). The membranes were blocked within 5% BSA in TBST for 1 h at RT and incubated overnight with following primary antibodies against HIF-1α (ab2185, Abcam), KIM-1 (AF1817, R&D Systems, Minneapolis, MN, USA), Alix (sc-53540, Santa Cruz Biotechnology, Dallas, TX), CD63 (sc-5275, Santa Cruz Biotechnology), TSG101 (ab30871, Abcam). Subsequently, corresponding HRP-conjugated secondary antibodies were applied to the samples. The proteins were probed through a hypersensitive ECL detection kit (BL520A, Biosharp, Hefei, China). Relative expression of objective proteins was normalized to β-actin (AB2001, Abways, Shanghai, China).

Statistical analysis

Data were presented as mean ± standard deviation. A two-tailed Student's *t*-test was applied to compare the difference between two groups. One-way ANOVA was conducted for comparison among three or more groups. All analyses were conducted by GraphPad Prism 8.0 software. A p value of less than 0.05 was considered statistically different.

ACKNOWLEDGMENTS

Supported by grants from the National Natural Science Foundation of China (Grant No. 82122011, 81970616, 81720108007, and 82030024).

AUTHOR CONTRIBUTIONS

J.C., J.C., Z.L., X.Z., and Y.W. conducted the experiments; J.C., T.T., and A.S. collected and analyzed the data; J.C., T.T., L.L., and B.L. designed the experiments and wrote the manuscript.

DECLARATION OF INTERESTS

The authors declare no conflicts of interests.

REFERENCES

1. Hoste, E.A.J., Kellum, J.A., Selby, N.M., Zarbock, A., Palevsky, P.M., Bagshaw, S.M., Goldstein, S.L., Cerdá, J., and Chawla, L.S. (2018). Global epidemiology and outcomes of acute kidney injury. Nat. Rev. Nephrol. *14*, 607–625.
2. James, M.T., Bhatt, M., Pannu, N., and Tonelli, M. (2020). Long-term outcomes of acute kidney injury and strategies for improved care. Nat. Rev. Nephrol. *16*, 193–205.
3. Lv, L.L., Feng, Y., Wu, M., Wang, B., Li, Z.L., Zhong, X., Wu, W.J., Chen, J., Ni, H.F., Tang, T.T., et al. (2020). Exosomal miRNA-19b-3p of tubular epithelial cells promotes M1 macrophage activation in kidney injury. Cell Death Differ. *27*, 210–226.
4. Matsushita, K., Saritas, T., Eiwaz, M.B., McClellan, N., Coe, I., Zhu, W., Ferdaus, M.Z., Sakai, L.Y., McCormick, J.A., and Hutchens, M.P. (2020). The acute kidney injury to chronic kidney disease transition in a mouse model of acute cardiorenal syndrome emphasizes the role of inflammation. Kidney Int. *97*, 95–105.
5. Nishikawa, H., Taniguchi, Y., Matsumoto, T., Arima, N., Masaki, M., Shimamura, Y., Inoue, K., Horino, T., Fujimoto, S., Ohko, K., et al. (2018). Knockout of the interleukin-36 receptor protects against renal ischemia-reperfusion injury by reduction of proinflammatory cytokines. Kidney Int. *93*, 599–614.
6. Sato, Y., Takahashi, M., and Yanagita, M. (2020). Pathophysiology of AKI to CKD progression. Semin. Nephrol. *40*, 206–215.
7. Liu, B.C., Tang, T.T., Lv, L.L., and Lan, H.Y. (2018). Renal tubule injury: a driving force toward chronic kidney disease. Kidney Int. *93*, 568–579.
8. Jia, Y., Zheng, Z., Xue, M., Zhang, S., Hu, F., Li, Y., Yang, Y., Zou, M., Li, S., Wang, L., et al. (2019). Extracellular vesicles from albumin-induced tubular epithelial cells promote the M1 macrophage phenotype by targeting Klotho. Mol. Ther. *27*, 1452–1466.
9. Karpman, D., Ståhl, A.L., and Arvidsson, I. (2017). Extracellular vesicles in renal disease. Nat. Rev. Nephrol. *13*, 545–562.
10. Borges, F.T., Melo, S.A., Özdemir, B.C., Kato, N., Revuelta, I., Miller, C.A., Gattone, V.H., 2nd, LeBleu, V.S., and Kalluri, R. (2013). TGF-beta1-containing exosomes from

injured epithelial cells activate fibroblasts to initiate tissue regenerative responses and fibrosis. J. Am. Soc. Nephrol. *24*, 385–392.

11. Lv, L.L., Feng, Y., Wen, Y., Wu, W.J., Ni, H.F., Li, Z.L., Zhou, L.T., Wang, B., Zhang, J.D., Crowley, S.D., and Liu, B.C. (2018). Exosomal CCL2 from tubular epithelial cells is Critical for albumin-induced tubulointerstitial inflammation. J. Am. Soc. Nephrol. *29*, 919–935.
12. Yeung, M.Y., McGrath, M., and Najafian, N. (2011). The emerging role of the TIM molecules in transplantation. Am. J. Transpl. *11*, 2012–2019.
13. Angiari, S., and Constantin, G. (2014). Regulation of T cell trafficking by the T cell immunoglobulin and mucin domain 1 glycoprotein. Trends Mol. Med. *20*, 675–684.
14. Ichimura, T., Bonventre, J.V., Bailly, V., Wei, H., Hession, C.A., Cate, R.L., and Sanicola, M. (1998). Kidney injury molecule-1 (KIM-1), a putative epithelial cell adhesion molecule containing a novel immunoglobulin domain, is up-regulated in renal cells after injury. J. Biol. Chem. *273*, 4135–4142.
15. van Timmeren, M.M., van den Heuvel, M.C., Bailly, V., Bakker, S.J.L., van Goor, H., and Stegeman, C.A. (2007). Tubular kidney injury molecule-1 (KIM-1) in human renal disease. J. Pathol. *212*, 209–217.
16. Yang, L., Brooks, C.R., Xiao, S., Sabbisetti, V., Yeung, M.Y., Hsiao, L.L., Ichimura, T., Kuchroo, V., and Bonventre, J.V. (2015). KIM-1-mediated phagocytosis reduces acute injury to the kidney. J. Clin. Invest. *125*, 1620–1636.
17. Mori, Y., Ajay, A.K., Chang, J.H., Mou, S., Zhao, H., Kishi, S., Li, J., Brooks, C.R., Xiao, S., Woo, H.M., et al. (2021). KIM-1 mediates fatty acid uptake by renal tubular cells to promote progressive diabetic kidney disease. Cell Metab. *33*, 1042–1061.e7. e7.
18. Xie, Y., Wang, Q., Wang, C., Qi, C., Ni, Z., and Mou, S. (2016). High urinary excretion of kidney injury molecule-1 predicts adverse outcomes in acute kidney injury: a case control study. Crit. Care *20*, 286.
19. Kobayashi, N., Karisola, P., Peña-Cruz, V., Dorfman, D.M., Jinushi, M., Umetsu, S.E., Butte, M.J., Nagumo, H., Chernova, I., Zhu, B., et al. (2007). TIM-1 and TIM-4 glycoproteins bind phosphatidylserine and mediate uptake of apoptotic cells. Immunity *27*, 927–940.
20. Matsumura, S., Minamisawa, T., Suga, K., Kishita, H., Akagi, T., Ichiki, T., Ichikawa, Y., and Shiba, K. (2019). Subtypes of tumour cell-derived small extracellular vesicles having differently externalized phosphatidylserine. J. Extracell. Vesicles *8*, 1579541.
21. Li, Z.L., Lv, L.L., Tang, T.T., Wang, B., Feng, Y., Zhou, L.T., Cao, J.Y., Tang, R.N., Wu, M., Liu, H., et al. (2019). HIF-1alpha inducing exosomal microRNA-23a expression mediates the cross-talk between tubular epithelial cells and macrophages in tubulointerstitial inflammation. Kidney Int. *95*, 388–404.
22. Feng, Y., Zhong, X., Tang, T.T., Wang, C., Wang, L.T., Li, Z.L., Ni, H.F., Wang, B., Wu, M., Liu, D., et al. (2020). Rab27a dependent exosome releasing participated in albumin handling as a coordinated approach to lysosome in kidney disease. Cell Death Dis. *11*, 513.
23. Gewin, L., Zent, R., and Pozzi, A. (2017). Progression of chronic kidney disease: too much cellular talk causes damage. Kidney Int. *91*, 552–560.
24. Han, W.K., Bailly, V., Abichandani, R., Thadhani, R., and Bonventre, J.V. (2002). Kidney Injury Molecule-1 (KIM-1): a novel biomarker for human renal proximal tubule injury. Kidney Int. *62*, 237–244.
25. Schmidt, I.M., Srivastava, A., Sabbisetti, V., McMahon, G.M., He, J., Chen, J., Kusek, J.W., Taliercio, J., Ricardo, A.C., Hsu, C.Y., et al. (2022). Plasma kidney injury molecule 1 in CKD: findings from the Boston kidney biopsy Cohort and CRIC studies. Am. J. Kidney Dis. *79*, 231–243.e1e1.
26. Ferenbach, D.A., and Bonventre, J.V. (2015). Mechanisms of maladaptive repair after AKI leading to accelerated kidney ageing and CKD. Nat. Rev. Nephrol. *11*, 264–276.
27. Hesp, A.C., Schaub, J.A., Prasad, P.V., Vallon, V., Laverman, G.D., Bjornstad, P., and van Raalte, D.H. (2020). The role of renal hypoxia in the pathogenesis of diabetic kidney disease: a promising target for newer renoprotective agents including SGLT2 inhibitors? Kidney Int. *98*, 579–589.
28. Lin, Q., Chen, Y., Lv, J., Zhang, H., Tang, J., Gunaratnam, L., Li, X., and Yang, L. (2014). Kidney injury molecule-1 expression in IgA nephropathy and its correlation with hypoxia and tubulointerstitial inflammation. Am. J. Physiol. Ren. Physiol. *306*, F885–F895.
29. Humphreys, B.D., Xu, F., Sabbisetti, V., Grgic, I., Movahedi Naini, S., Wang, N., Chen, G., Xiao, S., Patel, D., Henderson, J.M., et al. (2013). Chronic epithelial kidney injury molecule-1 expression causes murine kidney fibrosis. J. Clin. Invest. *123*, 4023–4035.
30. Gan, L., Liu, D., Xie, D., Bond Lau, W., Liu, J., Christopher, T.A., Lopez, B., Liu, L., Hu, H., Yao, P., et al. (2022). Ischemic Heart-derived small extracellular vesicles Impair Adipocyte function. Circ. Res. *130*, 48–66.
31. Huang, D., Sun, G., Hao, X., He, X., Zheng, Z., Chen, C., Yu, Z., Xie, L., Ma, S., Liu, L., et al. (2021). ANGPTL2-containing small extracellular vesicles from vascular endothelial cells accelerate leukemia progression. J. Clin. Invest. *131*, e138986.
32. Song, L., Tang, S., Han, X., Jiang, Z., Dong, L., Liu, C., Liang, X., Dong, J., Qiu, C., Wang, Y., and Du, Y. (2019). KIBRA controls exosome secretion via inhibiting the proteasomal degradation of Rab27a. Nat. Commun. *10*, 1639.
33. Yang, M.Q., Du, Q., Goswami, J., Varley, P.R., Chen, B., Wang, R.H., Morelli, A.E., Stolz, D.B., Billiar, T.R., Li, J., and Geller, D.A. (2018). Interferon regulatory factor 1-Rab27a regulated extracellular vesicles promote liver ischemia/reperfusion injury. Hepatology *67*, 1056–1070.
34. Kalluri, R., and LeBleu, V.S. (2020). The biology, function, and biomedical applications of exosomes. Science *367*, eaau6977.
35. Mathieu, M., Martin-Jaular, L., Lavieu, G., and Théry, C. (2019). Specificities of secretion and uptake of exosomes and other extracellular vesicles for cell-to-cell communication. Nat. Cell Biol. *21*, 9–17.
36. Mulcahy, L.A., Pink, R.C., and Carter, D.R.F. (2014). Routes and mechanisms of extracellular vesicle uptake. J. Extracell. Vesicles *3*, 24641.
37. Fuentes, P., Sesé, M., Guijarro, P.J., Emperador, M., Sánchez-Redondo, S., Peinado, H., Hümmer, S., and Cajal, S.R.Y. (2020). ITGB3-mediated uptake of small extracellular vesicles facilitates intercellular communication in breast cancer cells. Nat. Commun. *11*, 4730.
38. van Niel, G., D'Angelo, G., and Raposo, G. (2018). Shedding light on the cell biology of extracellular vesicles. Nat. Rev. Mol. Cell Biol. *19*, 213–228.
39. Ichimura, T., Asseldonk, E.J.P.V., Humphreys, B.D., Gunaratnam, L., Duffield, J.S., and Bonventre, J.V. (2008). Kidney injury molecule-1 is a phosphatidylserine receptor that confers a phagocytic phenotype on epithelial cells. J. Clin. Invest. *118*, 1657–1668.
40. Yamanishi, Y., Kitaura, J., Izawa, K., Kaitani, A., Komeno, Y., Nakamura, M., Yamazaki, S., Enomoto, Y., Oki, T., Akiba, H., et al. (2010). TIM1 is an endogenous ligand for LMIR5/CD300b: LMIR5 deficiency ameliorates mouse kidney ischemia/reperfusion injury. J. Exp. Med. *207*, 1501–1511.
41. Arai, S., Kitada, K., Yamazaki, T., Takai, R., Zhang, X., Tsugawa, Y., Sugisawa, R., Matsumoto, A., Mori, M., Yoshihara, Y., et al. (2016). Apoptosis inhibitor of macrophage protein enhances intraluminal debris clearance and ameliorates acute kidney injury in mice. Nat. Med. *22*, 183–193.
42. Kumar, A., Sundaram, K., Mu, J., Dryden, G.W., Sriwastva, M.K., Lei, C., Zhang, L., Qiu, X., Xu, F., Yan, J., et al. (2021). High-fat diet-induced upregulation of exosomal phosphatidylcholine contributes to insulin resistance. Nat. Commun. *12*, 213.
43. Su, H., Rustam, Y.H., Masters, C.L., Makalic, E., McLean, C.A., Hill, A.F., Barnham, K.J., Reid, G.E., and Vella, L.J. (2021). Characterization of brain-derived extracellular vesicle lipids in Alzheimer's disease. J. Extracell. Vesicles *10*, e12089.
44. Wang, X., Wilkinson, R., Kildey, K., Potriquet, J., Mulvenna, J., Lobb, R.J., Möller, A., Cloonan, N., Mukhopadhyay, P., Kassianos, A.J., and Healy, H. (2017). Unique molecular profile of exosomes derived from primary human proximal tubular epithelial cells under diseased conditions. J. Extracell. Vesicles *6*, 1314073.
45. Park, J.E., Dutta, B., Tse, S.W., Gupta, N., Tan, C.F., Low, J.K., Yeoh, K.W., Kon, O.L., Tam, J.P., and Sze, S.K. (2019). Hypoxia-induced tumor exosomes promote M2-like macrophage polarization of infiltrating myeloid cells and microRNA-mediated metabolic shift. Oncogene *38*, 5158–5173.
46. Yu, X., Deng, L., Wang, D., Li, N., Chen, X., Cheng, X., Yuan, J., Gao, X., Liao, M., Wang, M., and Liao, Y. (2012). Mechanism of TNF-alpha autocrine effects in hypoxic cardiomyocytes: initiated by hypoxia inducible factor 1alpha, presented by exosomes. J. Mol. Cell. Cardiol. *53*, 848–857.
47. Zahoor, M., Westhrin, M., Aass, K.R., Moen, S.H., Misund, K., Psonka-Antonczyk, K.M., Giliberto, M., Buene, G., Sundan, A., Waage, A., et al. (2017). Hypoxia promotes IL-32 expression in myeloma cells, and high expression is associated with poor survival and bone loss. Blood Adv. *1*, 2656–2666.

48. Tang, T.T., Wang, B., Li, Z.L., Wen, Y., Feng, S.T., Wu, M., Liu, D., Cao, J.Y., Yin, Q., Yin, D., et al. (2021). Kim-1 targeted extracellular vesicles: a new therapeutic Platform for RNAi to Treat AKI. J. Am. Soc. Nephrol. *32*, 2467–2483.

49. McCoy, I.E., Hsu, J.Y., Bonventre, J.V., Parikh, C.R., Go, A.S., Liu, K.D., Ricardo, A.C., Srivastava, A., Cohen, D.L., He, J., et al. (2022). Acute kidney injury Associates with long-term Increases in plasma TNFR1, TNFR2, and KIM-1: findings from the CRIC study. J. Am. Soc. Nephrol. *33*, 1173–1181.

50. Greenberg, J.H., Abraham, A.G., Xu, Y., Schelling, J.R., Feldman, H.I., Sabbisetti, V.S., Ix, J.H., Jogalekar, M.P., Coca, S., Waikar, S.S., et al. (2021). Urine biomarkers of kidney tubule health, injury, and inflammation are associated with progression of CKD in Children. J. Am. Soc. Nephrol. *32*, 2664–2677.

51. Tang, T.T., Wang, B., Wu, M., Li, Z.L., Feng, Y., Cao, J.Y., Yin, D., Liu, H., Tang, R.N., Crowley, S.D., et al. (2020). Extracellular vesicle-encapsulated IL-10 as novel nanotherapeutics against ischemic AKI. Sci. Adv. *6*, eaaz0748.